Interaction of Water Soluble Chitosan with Multiwalled Carbon Nanotubes

Wei Feng, Ying Li, and Peijun Ji
Dept. of Biochemical Engineering and Dept. of Chemical Engineering, Beijing University of Chemical Technology, Beijing, China

DOI 10.1002/aic.12562
Published online March 17, 2011 in Wiley Online Library (wileyonlinelibrary.com).

*A water soluble chitosan derivative (*p-*chitosan) was synthesized and used to functionalize multiwalled carbon nanotubes (MWCNTs) through the noncovalent interaction. The interaction of* p-*chitosan with MWCNTs was investigated by analyzing the spectra of ultraviolet-visible, Fourier transform infrared, Raman, and X-ray photoelectron. Circular dichroism spectroscopy was used to study the interaction as well. The results of the circular dichroism spectra indicate that, the interaction of* p-*chitosan with MWCNT makes* p-*chitosan less regularly structured. It was found that the interaction of* p-*chitosan with MWCNTs at a lower temperature is stronger than that at a higher temperature; pH conditions affect the interaction between* p-*chitosan and MWCNTs*. © 2011 American Institute of Chemical Engineers *AIChE J,* 58: 285–291, 2012
Keywords: multiwalled carbon nanotubes, chitosan, interaction

Introduction

Chitosan is a renewable resource and the second abundant polysaccharide present in nature.[1] Because of its versatile biological activity, excellent biocompatibility, and low toxicity, chitosan-based nanomaterials have been intensively explored for its application in pharmaceutical, biomedical, biotechnological, agricultural, food, and non-food industries,[2] as well as wastewater treatment.[3] Carbon nanotubes (CNTs) have extraordinary electrical, mechanical, and thermal properties and have the potential for a wide variety of applications.[4–7] The chitosan/CNT system is especially interesting because the introduced chitosan endows CNTs with biocompatibility.[8] Low molecular weight chitosan is covalently attached to multiwalled carbon nanotubes (MWCNTs),[9] and the MWCNTs can be dispersed in dimethylsulfoxide, dimethylformamide, dimethyl acetamide, and acetic acid aqueous solution. The chitosan derivatives 2-hydroxypropyltrimethylammonium chloride chitosan, carboxymethyl chitosan, and *N*-succinyl chitosan have been used to disperse CNTs in aqueous solutions.[8] The degree of deacetylation of chitosan has been evaluated for its effect on the dispersion of CNTs.[10] Chitosan and its derivatives have been studied for its dispersing of CNTs in solvents.[11,12] On the other hand, the conformation of chitosans on CNTs is very important for the application of the CNT composite.[13,14] Though chitosan/CNTs systems have been extensively studied, little research is reported for the interaction of chitosans with CNTs. In this article, the hydrophobically-modified chitosan, which is water soluble, is synthesized and applied to functionalize MWCNT. The interaction of *p*-chitosan with MWCNT will be investigated by analyzing the spectra of ultraviolet-visible (UV–vis), Fourier transform infrared (FTIR), Raman, and X-ray photoelectron (XPS). Circular dichroism (CD) spectroscopy is also used to study the interaction. The information will be useful to regulate and design the composite of chitosan/CNT.

Experimental

Materials

MWCNTs were purchased from Shenzhen Nanotech. Port. Co., China, and were purified according to the reported

Additional Supporting Information may be found in the online version of this article.

Correspondence concerning this article should be addressed to P. Ji at jipj@mail.buct.edu.cn.

procedures.[15] Chitosan, with a molecular weight of 10 kDa, was obtained from Jinan Haidebei Marine Bioengineering Co. (China). 1-(3-(dimethylamino)propyl)-3-ethylcarbodiimide hydrochloride (EDC), *N*-hydroxysulfosuccinimide (NHS), palmitic acid (99%), nitric acid (65.0–68.0 wt %), dimethyl sulfoxide (DMSO), acetone, ethanol, ether, sodium acetate, and acetic acid were purchased from Sigma-Aldrich Chemical Co., China.

Measurements

UV–vis spectra were recorded on a Shimadzu UV2550-PC spectrophotometer. FTIR spectra were recorded on a Fourier transform infrared spectrometer 3100 (Varian, USA) at room temperature and 2 cm^{-1} resolution. The crystalline structures of chitosan samples were analyzed by X-ray diffraction (XRD) (D/MAX 2500 VB2+/PC, Rigaku Corp., Tokyo, Japan) using CuKα radiation ($\lambda = 0.154$ nm) at 40 kV and 200 mA. Measurement was made using continuous scanning technique from 3 to 60° of 2θ at room temperature. Raman spectroscopy measurements were recorded using a Renishaw InVia equipment (514.5 nm, $E_{laser} = 2.41$ eV). Samples for the measurement of CD spectrum were prepared with a *p*-chitosan concentration of 0.2 mg/ml and a MWCNT concentration of 0.025 mg/ml. CD spectra (190–320 nm) were recorded on a JASCO J-810 CD instrument at temperatures 25, 40, 65, and 80°C. Cell length was 1.0 cm. Measurements were performed with a scanning speed of 1000 nm/min at a resolution of 1.0 nm. The spectra were corrected by subtracting the background of water or MWCNTs, and ten spectra were accumulated and averaged for each sample.

Synthesis of N-*palmitoyl chitosan (*p-*chitosan)*

Chitosan was refined twice by dissolving in 1% aqueous acetic acid solution followed by filtration to remove insoluble material. The soluble chitosan was precipitated with 1.0 M sodium hydroxide and then was washed thoroughly with deionized water. The precipitate was washed with ether and dried under vacuum at room temperature. Palmitic acid was grafted to chitosan by an EDC-mediated reaction through the formation of amide linkages. Chitosan (1.0 g) was dissolved in a buffer solution (40 ml, pH = 4.8) consisting of 0.1 M sodium acetate and 0.1 M acetic acid. A certain amount of palmitic acid dissolved in 50 ml of DMSO was added to the chitosan solution. The solution was cooled in an ice bath and followed by a dropwise addition of EDC and NHS. The mixture was kept stirring in an ice bath for 1 h. The molar ratio of EDC to palmitic acid was 1.5:1 and that of EDC to NHS was 5:1. After 24 h, the reaction mixture was poured into 200 ml of acetone/ammonia solution (7/3, v/v). The precipitate was filtered and washed thoroughly with acetone, ethanol, and ether. The precipitate was dried in vacuum at room temperature.

MWCNT attached with p-*chitosan*

Twenty milligrams of MWCNTs were added to an aqueous solution of *p*-chitosan (60 mg) dissolved in water (120 ml), followed by sonication for 1 h. The solution was centrifuged at 12,000 rpm for 30 min, yielding well-suspended MWCNTs with non-covalent *p*-chitosan coating. Unbound *p*-chitosan was thoroughly removed by repeated filtration through a 0.45 μm membrane and washing with water.

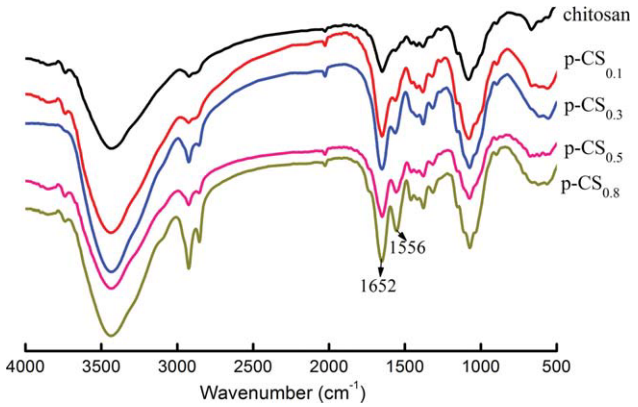

Figure 1. FTIR spectra of the chitosan and its derivatives, *p*-$CS_{0.1}$, *p*-$CS_{0.3}$, *p*-$CS_{0.5}$, and *p*-$CS_{0.8}$.

p-CS represents *p*-chitosan and the subscripts represent the initial ratio of palmitic acid to the glucosamine residue of chitosan (mol:mol). [Color figure can be viewed in the online issue, which is available at wileyonlinelibrary.com.]

Results and Discussion

Synthesis of N-*palmitoyl chitosan (*p-*chitosan)*

FTIR Analysis. The substitution of the *N*-acylated group to the amino group depends on the initial ratio of palmitic acid to the glucosamine residue of chitosan (mol:mol). In Figure 1 for the FTIR spectra, corresponding to the initial ratios 0.1, 0.3, 0.5, and 0.8, *p*-chitosans are designated as *p*-$CS_{0.1}$, *p*-$CS_{0.3}$, *p*-$CS_{0.5}$, and *p*-$CS_{0.8}$, respectively. The subscripts represent the initial ratio of palmitic acid to the glucosamine residue of chitosan. The broad band in the region of 3200–3500 cm^{-1} is attributed to the —NH_2 and —OH stretching vibrations. The bands at 1652 and 1556 cm^{-1} are assigned to the carbonyl stretching of amide I band and the N—H bending vibrations of amide II band, respectively.[16] With the increase of the initial ratio, the intensity of carbonyl stretching of amide I and the N—H bending vibrations of amide II increases. The results clearly reveal that *N*-acylated derivatives of chitosan were obtained. The prominent peaks at 2860–2972 cm^{-1} are assigned to the asymmetrical and symmetrical bending vibrations of —CH_2 groups,[16] which are because of the long chains grafted. It is noticeable that their intensity is obviously proportional to the degree of substitution.

^{1}H NMR Spectra. The ^{1}H NMR spectra of chitosan and *p*-chitosan (*p*-$CS_{0.3}$) are shown in Figure 2. For the chitosan, the peak at 1.99 ppm is because of the presence of the three *N*-acetyl protons of *N*-acetylglucosamine (GlcNAc) residue, and the peak at 2.94 ppm because of a H-2 proton of GlcNAc or glucosamine (GlcN) residues. Multiplets from 3.41 to 3.87 ppm correspond to the ring protons of GlcNAc or GlcN.[16] For the spectra of *p*-chitosan, the peak at 2.14 ppm is ascribed to the three *N*-acetyl protons of GlcNAc, and the peak at 3.08 ppm is because of an H-2 proton of GlcNAc or GlcN residues. The ring protons (H-3, 4, 5, 6, 6′) are considered to resonate at 3.46–3.78 ppm, peaks at 4.48 and 4.79 ppm are signs of H-1 overlapped with the sign of HOD.[16] Compared

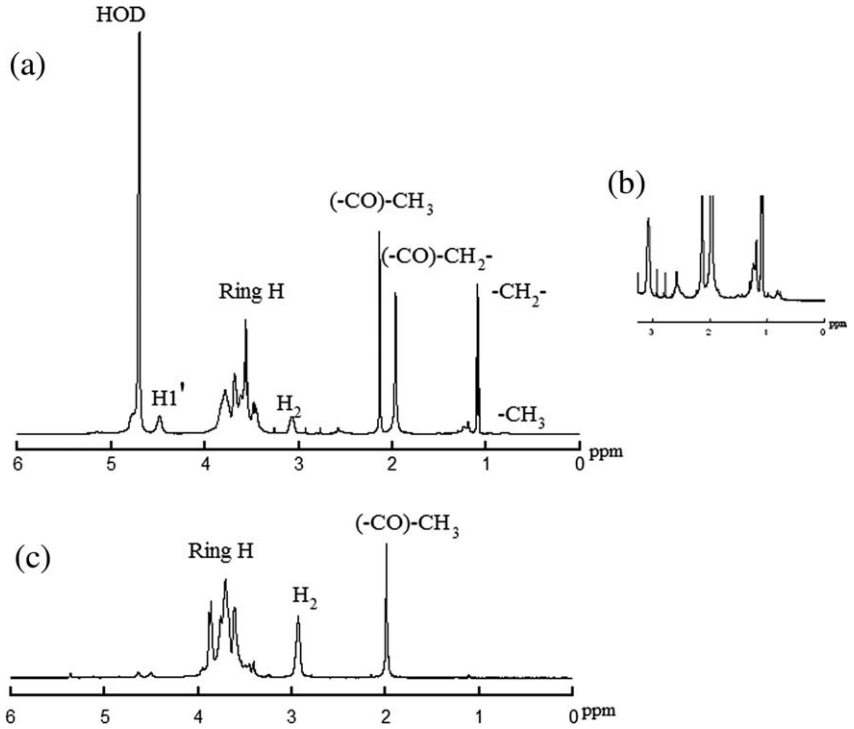

Figure 2. ^{1}H NMR spectrum of the *p*-chitosan (a); enlarged view of ^{1}HNMR spectrum of the *p*-chitosan from 0 ppm to 3.2 ppm (b); ^{1}HNMR spectrum of the chitosan (c).

with that of the chitosan, the spectra of the *p*-chitosan has some newly formed signals at 0.82, 1.09, and 1.97 ppm, which are ascribed to —CH_3, —CH_2—, and —CH_2—(CO) of the palmitoyl residue, respectively.[16] Compared to the signals of the chitosan, the signal shifts of the *p*-chitosan were because of the substitution of the *N*-acylated group to the amino group of the GlcN.[16] For *p*-$CS_{0.3}$, the degree of substitution is 11.6%, which is calculated based on the area at 0.82 and 3.08 ppm as illustrated in Figure 2B.

Solubility of the p-Chitosan in Aqueous Solution. The solubility of *p*-chitosan in deionized water and a buffer solution consisting of 0.1 M sodium acetate and 0.1 M acetic acid was measured. The measurement was carried out by adding 10 g sample in 10 ml water or buffer solution. As shown in Table 1, the solubility of *p*-chitosan depends on the degree of substitution of amine groups of the chitosan. The results indicate that the chitosan derivatives with more hydrophobic groups introduced or less —NH_2 groups substituted are not favored to have a good solubility both in water and in an acidic solution. The initial ratio of 0.3 is the most appropriate one for the synthesis of *p*-chitosan used to functionalize MWCNTs, as the synthesized *p*-chitosan at this initial ratio can be soluble well both in water and in an acidic solution.

X-Ray Diffraction Analysis. To determine the change of crystallinity of chitosan by N-acylation, the crystalline structures of the chitosan and the *p*-chitosan were examined by XRD, as shown in Figure 3. The diffraction pattern of the chitosan contains sharp, prominent signature peaks around $2\theta = 10.0$, 20.0, and 22.0°, as shown by the line in dark, indicating a high degree of crystallinity of the chitosan. While in the XRD patterns of *p*-$CS_{0.3}$, *p*-$CS_{0.5}$, and *p*-$CS_{0.8}$, the peak at $2\theta = 22°$ disappears. The peak sharpness at about $2\theta = 10.0°$ has been greatly reduced. With the increase of the N-acylation, the reflections around $2\theta = 20.0°$ become acute. Moreover, a new peak at $2\theta = 6°$ appears in the XRD pattern for *p*-$CS_{0.8}$, which indicates that new kind of crystallinity was formed because of the chemical modification. The structure of chitosan is stabilized by hydrogen bonding, whereas with some amine groups of chitosan substituted with palmitoyl groups, hydrophobic interactions between palmitoyl chains contribute to the formation of the crystalline structure of *p*-chitosan. However, the full width at half maximum is decreased from *p*-$CS_{0.3}$ to *p*-$CS_{0.8}$. It is meant that the amount of crystalline structure of *p*-$CS_{0.5}$ and that of *p*-$CS_{0.8}$ are larger than that of *p*-$CS_{0.3}$. The results are in accordance with the *p*-chitosan solubility

Table 1. Solubility of Chitosan and *p*-Chitosan at Neutral and Acid Conditions

Solvent	CS	*p*-$CS_{0.1}$	*p*-$CS_{0.2}$	*p*-$CS_{0.3}$	*p*-$CS_{0.4}$	*p*-$CS_{0.5}$	*p*-$CS_{0.8}$
Deionized water	n	n	p	y	p	n	n
Buffer solution (pH 4.8)	y	y	y	y	p	n	n

CS represents chitosan, *p*-CS represents *p*-chitosan, and the subscripts represent the initial ratio of palmitic acid to the glucosamine residue of chitosan (mol:mol).
y, Completely soluble; p, poorly soluble; n, insoluble.

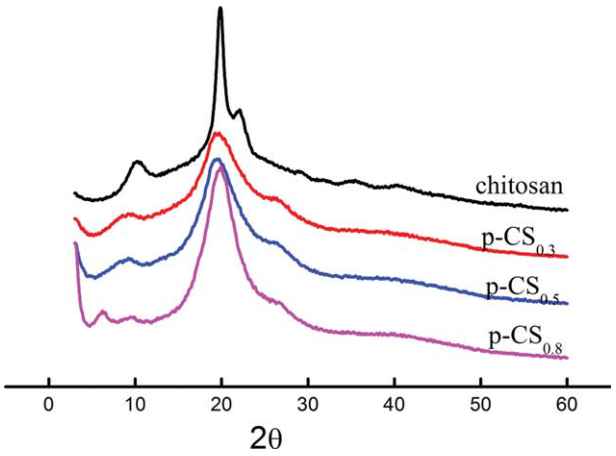

Figure 3. XRD patterns of chitosan derivatives, *p*-$CS_{0.3}$, *p*-$CS_{0.5}$, and *p*-$CS_{0.8}$.

p-CS represents *p*-chitosan and the subscripts represent the initial ratio of palmitic acid to the glucosamine residue of chitosan (mol:mol). [Color figure can be viewed in the online issue, which is available at wileyonlinelibrary.com.]

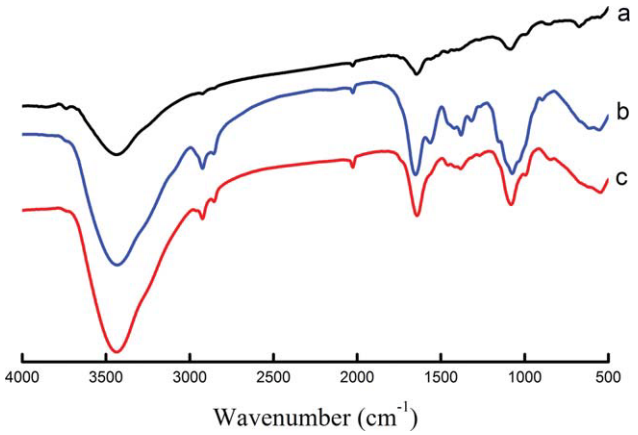

Figure 4. FTIR spectra of MWCNT (a), *p*-$CS_{0.3}$ (b), and *p*-chitosan/MWCNT (c).

[Color figure can be viewed in the online issue, which is available at wileyonlinelibrary.com.]

in water as presented in Table 1, which shows that *p*-$CS_{0.3}$ has a better solubility than other chitosan derivatives. So, *p*-$CS_{0.3}$ is chosen to functionalize MWCNTs. In the following sections, *p*-chitosan is referred to *p*-$CS_{0.3}$.

Interaction of MWCNT with p-*chitosan*

FTIR Analysis. As illustrated by the FTIR spectra in Figure 4, the MWCNT attached with the *p*-chitosan show the prominent peaks of the asymmetrical and symmetrical bending vibrations of —CH_2 groups at 2860–2972 cm^{-1},[16] which do not appear in the spectrum of MWCNT. *p*-Chitosan shows a strong absorption peak of carbonyl stretching of amide I at 1652 cm^{-1}.[16] This peak is reflected in the spectrum of *p*-chitosan/MWCNT. However, it shifts to 1643 cm^{-1} because of the interaction between the *p*-chitosan and MWCNT. The attachment of the *p*-chitosan on MWCNT is observed by high-resolution transmission electron microscopy (HRTEM) as indicated by arrows in Figure 5.

XPS Spectra Analysis. As can be seen in Figure 6A, the spectrum of the MWCNT shows the presence of carbon (95.65 at. %) and oxygen (4.35 at. %). The XPS survey spectrum of the MWCNT attached with the *p*-chitosan (Figure 6B) shows an increase of oxygen, attributed to the oxygen atoms in the *p*-chitosan. Moreover, the nitrogen in the *p*-chitosan is reflected in the spectrum. The detailed analysis for the peaks is presented in Supporting Information Figures S1–S3. The XPS spectra confirm the attachment of the *p*-chitosan on MWCNT.

Raman Spectra Analysis. The attachment of the *p*-chitosan to the surface of MWCNTs can be seen from Raman spectra. The G-band, in the 1500–1600 cm^{-1} region, results from the tangential C—C stretching vibrations both longitudinally and transversally on the carbon nanotube axis.[17,18] In the spectrum of MWCNTs, the G-band peaks at 1578 cm^{-1}. In the presence of *p*-chitosan coating, this band shifts by 6 cm^{-1} from 1578 to 1584 cm^{-1} (Figure 7). The disorder peak, also known as the D-band, can be found in the 1300–1400 cm^{-1} region.[17] This peak is attributed to scattering from sp2 carbons containing defects. The strength of this peak is

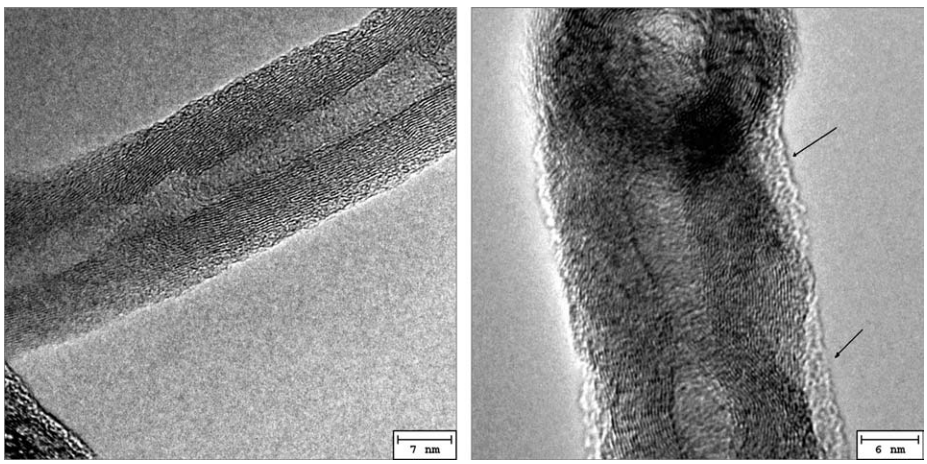

Figure 5. HRTEM image of purified MWCNT (left) and MWCNT attached with the *p*-chitosan as indicated by arrows (right).

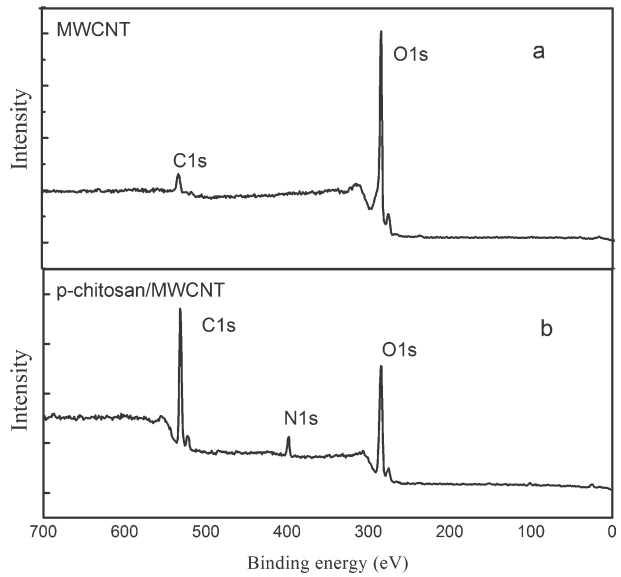

Figure 6. XPS survey spectra of MWCNT (composition: 95.65 at. % C, 4.35 at. % O) and *p*-chitosan/MWCNT (composition: 68.87 at. % C, 25.42 at. % O, 5.72 at. % N).

related to the amount of disordered graphite and the degree of conjugation disruption in the graphene sheet.[17,18] The D-band of MWCNTs peaks at 1347 cm^{-1}. It is noted that, in the presence of the *p*-chitosan coating, the D-band shifts by 10 cm^{-1} from 1347 to 1357 cm^{-1}. The strong interactions between the *p*-chitosan and the nanotubes increase the energy necessary for vibrations and shift the Raman band to the higher frequency.[19] The results of the D- and G-bands indicate the attractive interaction between the *p*-chitosan and the graphite sheet.[17]

UV–Vis Spectra. The *p*-chitosan solution was prepared by dissolving 60 mg of *p*-chitosan in 120 ml of water. This *p*-chitosan solution was used as the starting solution for preparing the *p*-chitosan solutions with difference pH values. Twenty milligrams of MWCNT was added into the neutral *p*-chitosan solution. The dispersion of MWCNTs was carried

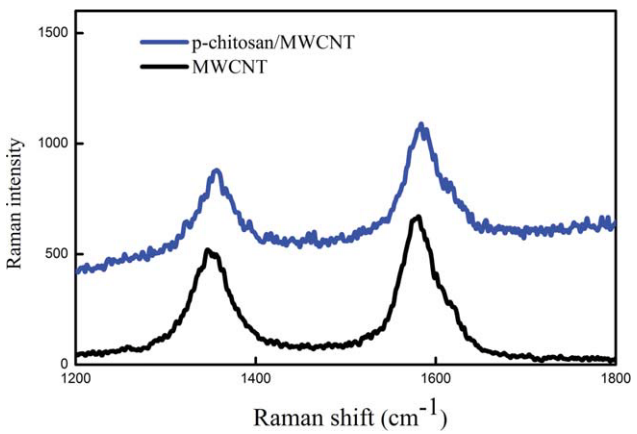

Figure 7. Raman spectra of *p*-chitosan/MWCNT and MWCNT.

[Color figure can be viewed in the online issue, which is available at wileyonlinelibrary.com.]

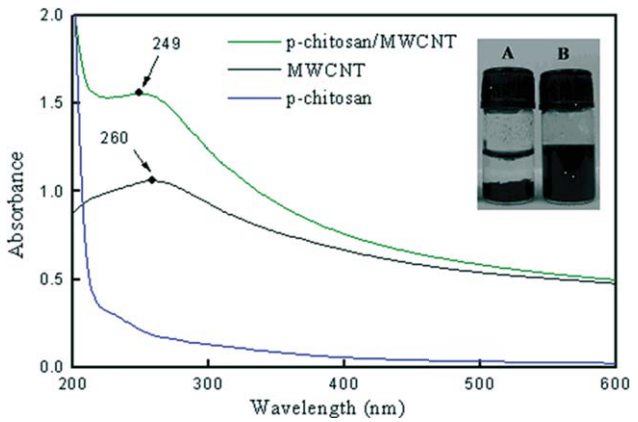

Figure 8. UV–vis absorbance of *p*-chitosan/MWCNT, MWCNT, and *p*-chitosan.

The insert: (a) MWCNTs in water and (b) *p*-chitosan/MWCNTs in water. [Color figure can be viewed in the online issue, which is available at wileyonlinelibrary.com.]

out under sonication. After centrifugation, the suspension was monitored with UV–vis spectroscopy. Figure 8 shows the UV–vis spectra of *p*-chitosan/MWCNT, MWCNT, and *p*-chitosan. The MWCNT has a characteristic peak at 260 nm, this peak shifts to 249 nm after the *p*-chitosan attached onto the MWCNT. The peak shift is ascribed to the interaction between the *p*-chitosan and the MWCNT. The insert indicates that the MWCNTs functionalized with the *p*-chitosan have a good dispersity in water.

Circular Dichroism Spectra. CD spectroscopy was applied to study the interaction of *p*-chitosan with MWCNT in aqueous solutions at different pH conditions and temperatures. The CD spectra of *p*-chitosan in aqueous solution has a broad negative CD band, corresponding to $n \rightarrow \pi^*$ electronic transition of the —NH—CO— chromophore of GlcNAc units located at about 210 nm, this band position is independent of pH and ionic strength.[20] For a polymer, the peak intensity of a CD spectrum depends on the structural regularity of the polymer.[21] The more regularly structured polymer will have a larger intensity of CD spectrum.[21] When the *p*-chitosan interacting with MWCNT, the intermolecular interaction between the *p*-chitosan molecules decreases. As a consequence, the *p*-chitosan is less regularly structured, as schematically illustrated in Figure 9. This results in that the intensity of CD spectrum of free *p*-chitosan is larger than that of the *p*-chitosan interacting with MWCNT, as presented in Figure 10, which shows the CD spectra of *p*-chitosan/MWCNT and that of free *p*-chitosan at different temperatures. The intensity difference between free *p*-chitosan and the *p*-chitosan interacting with MWCNT is affected by temperature. The observed experimental results (Figure 10) show that, at a higher temperature, the intensity of CD spectrum of the *p*-chitosan interacting with MWCNT is more close to that of free *p*-chitosan. The intensity difference of CD spectra becomes smaller with the increase of temperature. The results of the intensity difference of CD spectra indicate that, at a higher temperature, the interaction of *p*-chitosan with MWCNT is decreased. The reason can be explained by the following. The *p*-chitosan contains hydroxyl and amino groups as well as hydrophobic chains. It

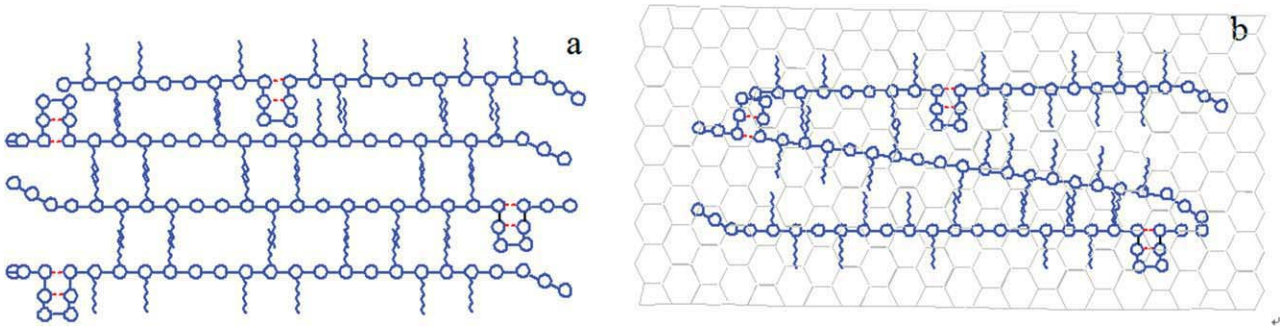

Figure 9. Representation of free *p*-chitosan (regularly structured) (a) and the *p*-chitosan (less regularly structured) interacting with MWCNT (b).

The red doted lines indicate the hydrogen bonding interaction. [Color figure can be viewed in the online issue, which is available at wileyonlinelibrary.com.]

can interact with the MWCNT by multiple interactions, including hydrophobic interactions, interactions via hydroxyl and amino groups through defect sites of the nanotubes (usually COOH). Where as, these types of interactions decrease with the increase in temperature.

Figure 11 shows CD spectra of free *p*-chitosan and the *p*-chitosan interacting with MWCNT at different pH conditions. As can be seen, the peak intensity difference between free *p*-chitosan and the *p*-chitosan interacting with MWCNT at the acidic and basic conditions are larger than that at the neutral condition. This can be explained that, at the acidic and basic conditions, the intramolecular hydrogen bonding interactions are reduced, and the interaction of *p*-chitosan with MWCNT is facilitated. The stronger interaction at the acidic and basic conditions makes the intensity difference become larger.

Conclusions

Chitosan derivatives were synthesized with different initial ratios of palmitic acid to the glucosamine residue of chitosan (mol:mol). It was found that the chitosan derivative synthesized with the initial ratio of 0.3 is the most appropriate one in terms of solubility in aqueous solutions. The *p*-chitosan was used to functionalize MWCNTs through a non-covalent interaction. The spectra of UV–vis, FTIR, Raman, and XPS were analysed to investigate the interaction of the *p*-chitosan

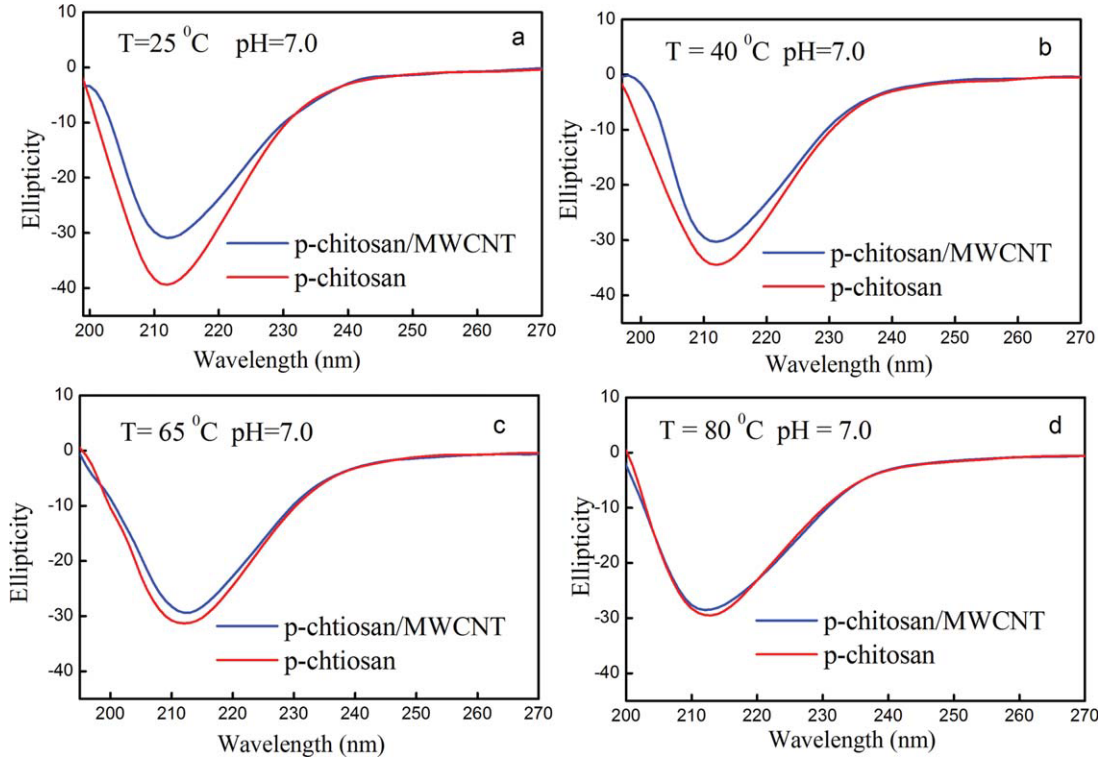

Figure 10. CD spectra of the *p*-chitosan interacting with MWCNT and free *p*-chitosan at different temperature.

[Color figure can be viewed in the online issue, which is available at wileyonlinelibrary.com.]

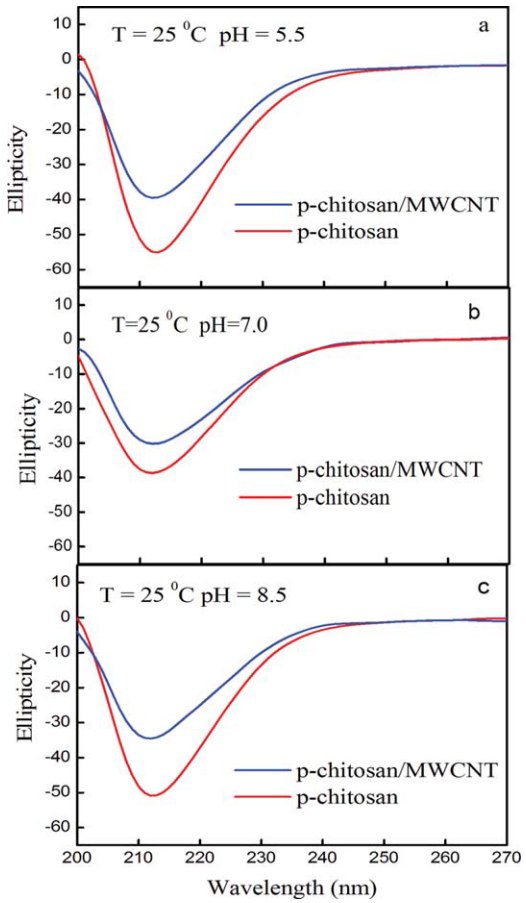

Figure 11. CD spectra of the *p*-chitosan and *p*-chitosan/MWCNT at different pH values.

[Color figure can be viewed in the online issue, which is available at wileyonlinelibrary.com.]

with MWCNTs. The CD spectra indicate that, when interacting with MWCNT, the *p*-chitosan is not as regularly structured as that of free *p*-chitosan. The interaction of the *p*-chitosan with MWCNTs at a lower temperature is stronger than that at a higher temperature. The interaction of the *p*-chitosan with MWCNTs at the acidic and basic conditions is stronger than that at a neutral condition.

Acknowledgments

This work was supported by the National Science Foundation of China (21076018), the National Basic Research Program of China (2007CB714302, 2011CB200905), the 863 program (2009AA033001), and the Program for New Century Excellent Talents in University.

Literature Cited

1. Ravi Kumar M, Muzzarelli R, Muzzarelli C, Sashiwa H, Domb A. Chitosan chemistry and pharmaceutical perspectives. *Chem Rev*. 2004;104:6017–6084.
2. Mourya VK, Inamdar NN. Chitosan-modifications and applications: opportunities galore. *React Funct Polym*. 2008;68:1013–1051.
3. Chatterjee S, Lee MW, Woo SH. Adsorption of congo red by chitosan hydrogel beads impregnated with carbon nanotubes. *Bioresour Technol*. 2010;101:1800–1806.
4. Zhang P, Henthorn DB. Synthesis of PEGylated single wall carbon nanotubes by a photoinitiated graft from polymerization. *AIChE J*. 2010;56:1610–1615.
5. Ozarkar S, Jassal M, Agrawal AK. Improved dispersion of carbon nanotubes in chitosan. *Fiber Polym*. 2008;9:410–415.
6. Liu Y, Tang J, Chen X, Xin JH. Decoration of carbon nanotubes with chitosan. *Carbon*. 2005;43:3178–3180.
7. Wu Z, Feng W, Feng Y, Liu Q, Xu X, Sekino T, Fujii A, Ozaki M. Preparation and characterization of chitosan-grafted multiwalled carbon nanotubes and their electrochemical properties. *Carbon*. 2007;45:1212–1218.
8. Zhang J, Wang Q, Wang L, Wang A. Manipulated dispersion of carbon nanotubes with derivatives of chitosan. *Carbon*. 2007;45:1911–1920.
9. Ke G, Guan W, Tang C, Guan W, Zeng D, Deng F. Covalent functionalization of multiwalled carbon nanotubes with a low molecular weight chitosan. *Biomacromolecules*. 2007;8:322–326.
10. Iamsamai C, Hannongbua S, Ruktanonchai U, Soottitantawat A, Dubas ST. The effect of the degree of deacetylation of chitosan on its dispersion of carbon nanotubes. *Carbon*. 2010;48:25–30.
11. Yan LY, Poon YF, Chan-Park MB. Individually dispersing single-walled carbon nanotubes with novel neutral pH water-soluble chitosan derivatives. *J Phys Chem C*. 2008;112:7579–7587.
12. Shieh YT, Wu HM, Twu YK. An investigation on dispersion of carbon nanotubes in chitosan aqueous solutions. *Colloid Polym Sci*. 2010;288:377–385.
13. Pauliukaite R, Ghica M, Fatibello-Filho O, Brett C. Comparative study of different cross-linking agents for the immobilization of functionalized carbon nanotubes within a chitosan film supported on a graphite-epoxy composite electrode. *Anal Chem*. 2009;81:5364–5372.
14. Hu Y, Chen W, Lu L, Liu J, Chang C. Electromechanical actuation with controllable motion based on a single-walled carbon nanotube and natural biopolymer composite. *Acs NANO*. 2010;4:3498–3502.
15. Liu J, Rinzler AG, Dai H, Hafner JH, Bradley RK, Boul PJ, Lu A, Iverson T, Shelimov K, Huffman CB, Rodriguez-Macias F, Shon YS, Lee TR, Colbert DT, Smalley RE. Fullerene pipes. *Science*. 1998;280:1253–1256.
16. Tien CL, Lacroix M, Ispas-Szabo P, Mateescu MA. *N*-acylated chitosan: hydrophobic matrices for controlled drug release. *J Controlled Release*. 2003;93:1–13.
17. Sinani VA, Gheith MK, Yaroslavov AA, Rakhnyanskaya AA, Sun K, Mamedov AA, Wicksted JP, Kotov NA. Aqueous dispersions of single-wall and multiwall carbon nanotubes with designed amphiphilic polycations. *J Am Chem Soc*. 2005;127:3463–3472.
18. Holzinger M, Abraham J, Whelan P, Graupner R, Ley L, Hennrich F, Kappes M, Hirsch A. Functionalization of single-walled carbon nanotubes with (R-)oxycarbonyl nitrenes. *J Am Chem Soc*. 2003;125:8566–8580.
19. Nepal D, Geckeler KE. pH-sensitive dispersion and debundling of single-walled carbon nanotubes: lysozyme as a tool. *Small*. 2006;2:406–412.
20. Miura Y, Yasuda K, Yamamoto K, Koike M, Nishida Y, Kobayashi K. Inhibition of Alzheimer amyloid aggregation with sulfated glycopolymers. *Biomacromolecules*. 2007;8:2129–2134.
21. Gao XY, Xing GM, Yang YL, Shi XL, Liu R, Chu WG, et al. Detection of trace Hg^{2+} via induced circular dichroism of DNA wrapped around single-walled carbon nanotubes. *J Am Chem Soc*. 2008;130:9190–9191.

Manuscript received Sep. 5, 2010, revision received Nov. 1, 2010, and final revision received Jan. 13, 2011.